DOI: 10.24996/ ijs.2017.58.4B.26

Iraqi Journal of Science

ISSN: 0067-2904

A Comprehensive Case Study of a Frontal Mineral Dust Storm in spring over Iraq

Thaer O. Roomi*, Khawla N. Zeki, Ahmed F. Hassoon
Department of Atmospheric Sciences, College of Science, University of Almustansiriyah, Baghdad, Iraq.

Abstract

Dust storms are among the most important weather phenomena in Middle East. The Shamal dust storms are dominated across Iraq and the whole Middle East, especially in summer. However, frontal type of dust storms is possible in winter and spring. In this research, a comprehensive case study was conducted to a dust storm that occurred on 20 March 2016 from many perspectives: synoptic, satellite imagery, dust concentration analysis, visibility reduction, and aerosol optical depth. The study shows that the dust storm initiated inside Syria and moved eastward with the movement of the front. Dust concentrations and aerosol optical depth were also discussed that simulate the dust storm over Iraq in a reasonable way with some differences. The dust concentrations values increase gradually during the early hours of 20 March at 1200 UTC to become within (200-5000) $\mu g/m^3$. The dust concentrations comparison with some surrounding countries shows that Iraq had the maximum value at the dust storm time. An experimental relationship to calculate the dust concentration from visibility was tested according to the multi-model products and revealed acceptable estimates. Dust aerosol optical depth offers good means to quantify the dust amount in the Middle East where the dust is the determining factor. Additional investigation was done by using the relative vorticity and the potential vorticity. The results of this investigation show that there are upper shortwaves that are responsible of strengthening of the low pressure system at the surface. The computed value of potential vorticity advection was estimated to be about (2.7×10-4 K m2/kg s) along a distance of about 500 km which suggested a high value of divergence east of the system which lead to a significant updraft.

Keywords: Mineral dust; Dust storms; Frontal dust storms; Dust concentrations; Aerosol optical depth.

دراسة حالة شاملة لعاصفة غبار معدني جبهوية في الربيع فوق العراق

ثائر عبيد رومي*، خولة نهاد زكي، أحمد فتاح حسون
قسم علوم الجو، كلية العلوم، الجامعة المستنصرية، بغداد، العراق.

الخلاصة

العواصف الغبارية هي واحدة من أهم الظواهر الطقسية في الشرق الأوسط. وتعتبر عواصف الشمال الغبارية هي السائدة في العراق والشرق الأوسط بأكمله وخاصة في الصيف. على اية حال، العواصف الغبارية من النوع الجبهوي تكون محتملة الحدوث في الشتاء والربيع. في هذا البحث، تم اجراء حالة دراسية شاملة على عاصفة غبارية حدثت في يوم 20 آذار 2016 من عدة جوانب: ساينوبتيكية، صور اقمار اصطناعية، تحليل تراكيز الغبار، تردي مدى الرؤية، والعمق البصري للعوالق. الدراسة اظهرت بان العاصفة الغبارية ابتدأت داخل

*Email: th.roomi.atmsc@uomustansiriyah.edu.iq

سوريا وتحركت شرقاً مع حركة الجبهة. تركيز الغبار والعمق البصري للعوالق تم مناقشتها والتي كانت تحاكي العاصفة الغبارية فوق العراق بشكل مقبول مع بعض الاختلافات. قيم تراكيز الغبار تزداد تدريجياً خلال الساعات المبكرة من 20 آذار عند الساعة 1200 بالتوقيت العالمي لتصبح ضمن 200−5000 مايكروغرام بالمتر المكعب. أظهرت مقارنة تراكيز الغبار مع بعض الدول المحيطة بأن للعراق اعلى قيمة تركيز خلال وقت العاصفة الغبارية. كما تم اختبار علاقة تجريبية لحساب تركيز الغبار من مدى الرؤية طبقاً الى مخرجات لنماذج مختلفة واظهر تخمينات مقبولة. العمق البصري لعوالق الغبار يوفر وسيلة جيدة لتحديد كمية الغبار في الشرق الأوسط حيث يعتبر الغبار عاملا محدداً. استقصاء اضافي تم عمله باستخدام الدردورية النسبية والدردورية الجهدية. نتائج هذا الاستقصاء بينت بان هناك موجات قصيرة علوية مسؤولة عن تقوية نظام المنخفض الجوي عند السطح. القيمة المقاسة لتأفق الدردورية الجهدية خمنت بحوالي (2.7×10−4 K m2/kg s) على طول مسافة ما يقارب 500 كيلومتر التي تقترح قيمة عالية للتباعد شرق النظام والتي تقود الى عملية رفع كبيرة.

Introduction

Mineral dust is a significant contributor to atmospheric aerosol [1]. It affects: health [2], horizontal visibility [3], transportation, agriculture, cloud nucleation, solar economy, nutrition for terrestrial and marine ecosystems [4], and significantly reduces the air quality [5]. On account of its optical properties and its mineral composition, it influences directly the atmosphere's radiation budget [6]. Hence, it generally plays a cooling effect since it reflects the radiation back to the space and may reduce the efficiency of solar devices [7]. Changes in radiative forcing have an effect on the monsoonal circulation and such changes induced by dust storms can have a major influence on the strength of the monsoon which in turn plays an important role in climate and weather of Middle East [8].

Mineral dust is a dominant atmospheric aerosol and is contributing more than half of the total global aerosol burden [9]. A dust storm is internationally defined as a dust-raising event that reduces visibility to below 1000 m [10]. Dust storms form in semi-arid and arid regions where small dust (and sand) particles are literally blown through the air. The dust production mechanism is based on the viscous/turbulent mixing, shear-free convection diffusion, and soil moisture [11]. Dust particles are small enough to be lifted aloft by currents of turbulent air and carried into suspension [12]. Although the pressure pattern is favorable for raising dust into the atmosphere, it appears that the influx of cool air aloft adds to the effects of the strong surface heating. Ginoux *et al*. [13] assume all topographic lows with bare ground surface to have accumulated sediments which are potential dust sources.

Horizontal pressure gradients in the existence of depression play an important role in generating dust storm [14]. This steepens the lapse rate and creates the instability necessary for lifting dust particles and keeping them suspended. Soil has three main size sets according to diameters, clay (<2 microns), silt (2-74 microns), sand (>74 microns) [15]. Dust and size with the strength of the wind required to lift dust into the atmosphere control the amount and duration of dust storm. The uplifting of particles smaller than 0.1 microns by air is limited by the adhesive and cohesive forces which tend to form larger particles or aggregates [13].

Dust storms lift millions of tons of dust into the atmospheric boundary layer [16]. Their estimated global emission ranging from 1000 to 3000 Mt yr^{-1}, and an average atmospheric dust load ranging from 8 to 35 Mt yr^{-1} [9].

Dust is moved by the prevailing winds and transported vertically by convective processes, as well as adiabatic vertical motion related with frontal systems. Atmospheric dust settles on the Earth's surface through both molecular and gravitational settling (dry deposition) and wet deposition with precipitation [17].

Many studies have been conducted to investigate the dust storms in Iraq. For instance, Omar Khaleed (in 2009) carried out a study to identify the sources of dust storms in Iraq and the surrounding countries by using factor analysis of aerosols data (aerosols index) and satellite infrared and visible images. It was found that the aerosols index is ranging from 40 in the northern area to 50 in the southern area of Iraq [18]. Another research work was done by Muhanad Khudur (in 2014) focused on the study of the impact of dust phenomena on solar energy that received in Iraq and its effect on the solar systems [19]. Sama Al-Dabbagh (in 2015) used BSC-DREAM8b model to simulate dust outbreaks cases. The results of the study are evaluated to verify the model performance [20].

In this paper, a dust storm case study which happened on the morning of 20 March 2016 was comprehensively discussed. The study dealt with the dust storm from many aspects: synoptic analysis, satellite imagery, dust concentration analysis, visibility reduction, and dust aerosols optical depth analysis.

Major dust storm in Iraq and Arabian Peninsula

Iraq is one of the most affected countries in the Middle East concerning the occurrences of dust storms and it is also an important source of dust storm north of Arabian Peninsula (AP) [21]. The Ministry of Environment, in Iraq recorded 122 dust storms and 283 dusty days, and sources suggest that within the next ten years Iraq could witness 300 dusty days and dust storms per year [12]. MODIS satellite images between 2003 and 2011 showed that nearly 60 dust storms occurred in the Middle East. Amongst these, 48 dust storms were just spread over Iraq. The analysis of the MODIS satellite images showed that the dust storms from the Tigris-Euphrates alluvial plain may affect more than 10 countries in the Middle East [22].

Generally, in the Middle East, dust activity peaks in the late spring and summer and being minimum in the winter [22, 23]. The results which were presented by Kutiel and Furman [7] placed the Middle East as one of the regions most affected by dust in the world, next to Africa. Eastern Syria, northern Jordan, and western Iraq are the sources for most of the fine dust particles found in the Middle East dust storms [24].

The climate in West Asia (including AP) is largely influenced by three pressure systems: the Siberian anticyclone in winter over central Asia; the monsoon depression in summer over the Indian subcontinent; and the low pressures coming from the Mediterranean Sea in winter and spring [17].

Although dust storms can take a variety of shapes and forms, there are three main types: Shamal, frontal, and convective. The most common type across the Arabian Peninsula (AP) is the Shamal, which is a strong north-northwesterly wind, capable of lifting dust from the Tigris-Euphrates basin and transporting it to the Persian Gulf and other parts of AP [25]. In summer, this Shamal wind is strong and causes surface dust emission which can last for several days in a row, strengthening during the day and weakening at night. In fact Shamal dust storms can happen all over the year, including the winter [26]. The dust storms caused by frontal system have still been less studied than the shamal dust storms. These storms are common in winter and spring and primarily triggered by dynamical lifting, which is related to cold fronts and their associated mid-latitude troughs; in contrast to summer, where dust storms are related to the diurnal vertical mixing, which is related to solar heating [27]. The standard mid-latitude cold frontal system associated with strong pressure gradients that progressively move across the AP and endure for 24-36 hours [28]. The frontal dust storm is on a larger scale than others. It is a dynamic synoptic system that mixes the dust in the air and carries it for great distances [15].

Methodology

Iraq is located in the northeast of the Arabian Peninsula (AP) and has a 39% of its area as a desert [29]. The AP is surrounded from the north by Taurus Mountains, and Zagreus Mountains from west of Iran. For the Saudi Arabian region, the Jordanian and Syrian mountains lie to the northwest, the Al Hijas and Asir ranges to the southwest, while the Hadramaunt Mountains lie to the southeast [30]. The lack of precipitation in the inland regions of the AP provide a suitably dry surface region comprised of sand, clay and fine silt, ideal for the formation of dust storms [28]. In Figure-1, Region 1 is the Fertile Crescent region that located between Tigris and Euphrates river deltas and flood plains. The Fertile Crescent is a source region comprised of alluvial fans and dry flood plains containing a mixture of clay and silt particles [30].

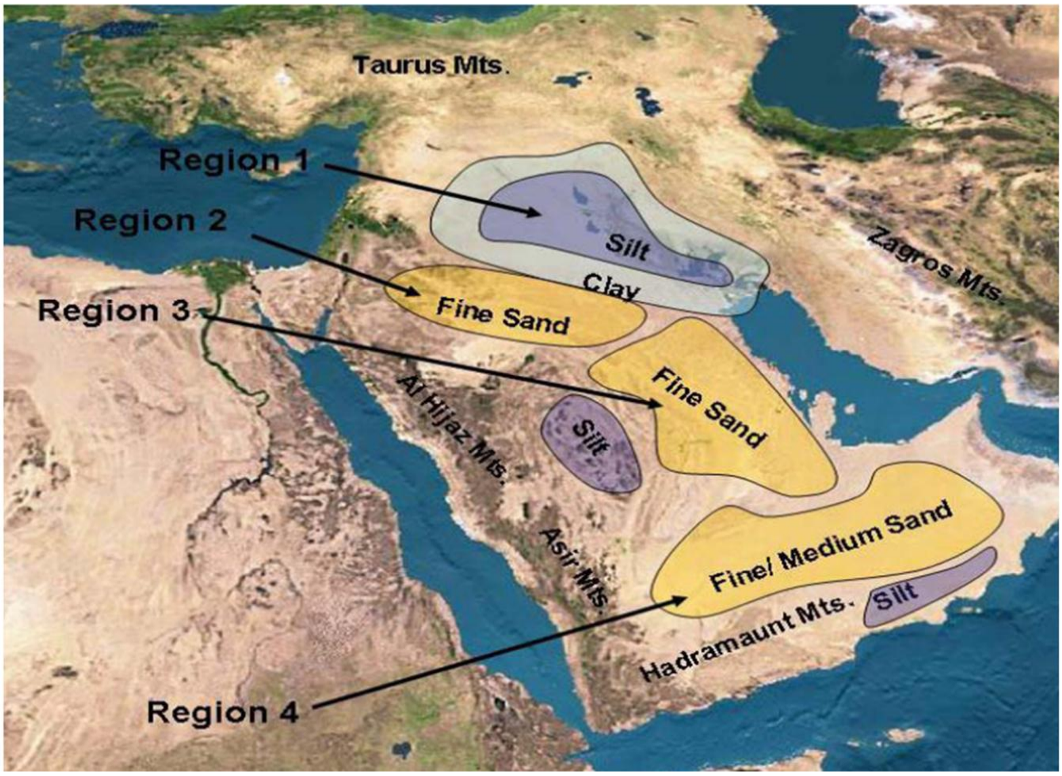

Figure1- Arabian Peninsula dust sources [30].

In this paper, a study case of a severe dust storm which broke out in a large area of Iraq in the early hours of 20 March 2016 was discussed comprehensively. By considering the unique conditions of the different regions regarding the synoptic features associated with dust events, the dust storm was investigated from many perspectives: synoptic, dust concentration analysis, aerosol optical depth, and satellite imagery. The visibility reduction during this event had reduced to less than 100 m before it gradually improved at afternoon.

The way which will be adopted to in this work comprises many aspects: Synoptic analysis of the meteorological data and pressure systems, weather imagery, discussion of aerosol optical depth and concentrations, visibility reduction, and vorticity.

Results and Discussion

In the analysis of this storm, it is important to first look one day ahead of the onset of blowing dust and a day after in order to track the synoptic situation leading up to the event.

A. Synoptic Analysis

Figure-2 shows graphs of the hourly soundings of sea surface pressure, air temperature, and wind speed, respectively of Baghdad weather station within three days, 19, 20, and 21 March 2016. The first graph of sea surface pressure Figure2- (a) clearly shows a discontinuously trend of a small increase followed with noticeable decrease at 0900 UTC on 20 March. On the other hand, temperature graph Figure 2-(b) indicated a sudden drop of about 4^{o}C at 0900 UTC on 20 March which corresponded with the passing of a cold front. The last graph of wind speed Figure 2-(c) clearly depicted the increasing of the wind speed that reached a maximum of 12 knots at the time the cold front during passing over Baghdad (about 0900 UTC) on 20 March. The existence of a frontal system is essential to emit the dust at the cases which include not very high wind speed. All these graphs suggested a cold front passage. The dust storm was prefrontal type since it happened in advance to the front passage over Baghdad at 0900 UTC. The dust was initiated over the Syrian Desert before crossing the Iraqi borders with a cyclonic activity of the low pressure system as will be explained later.

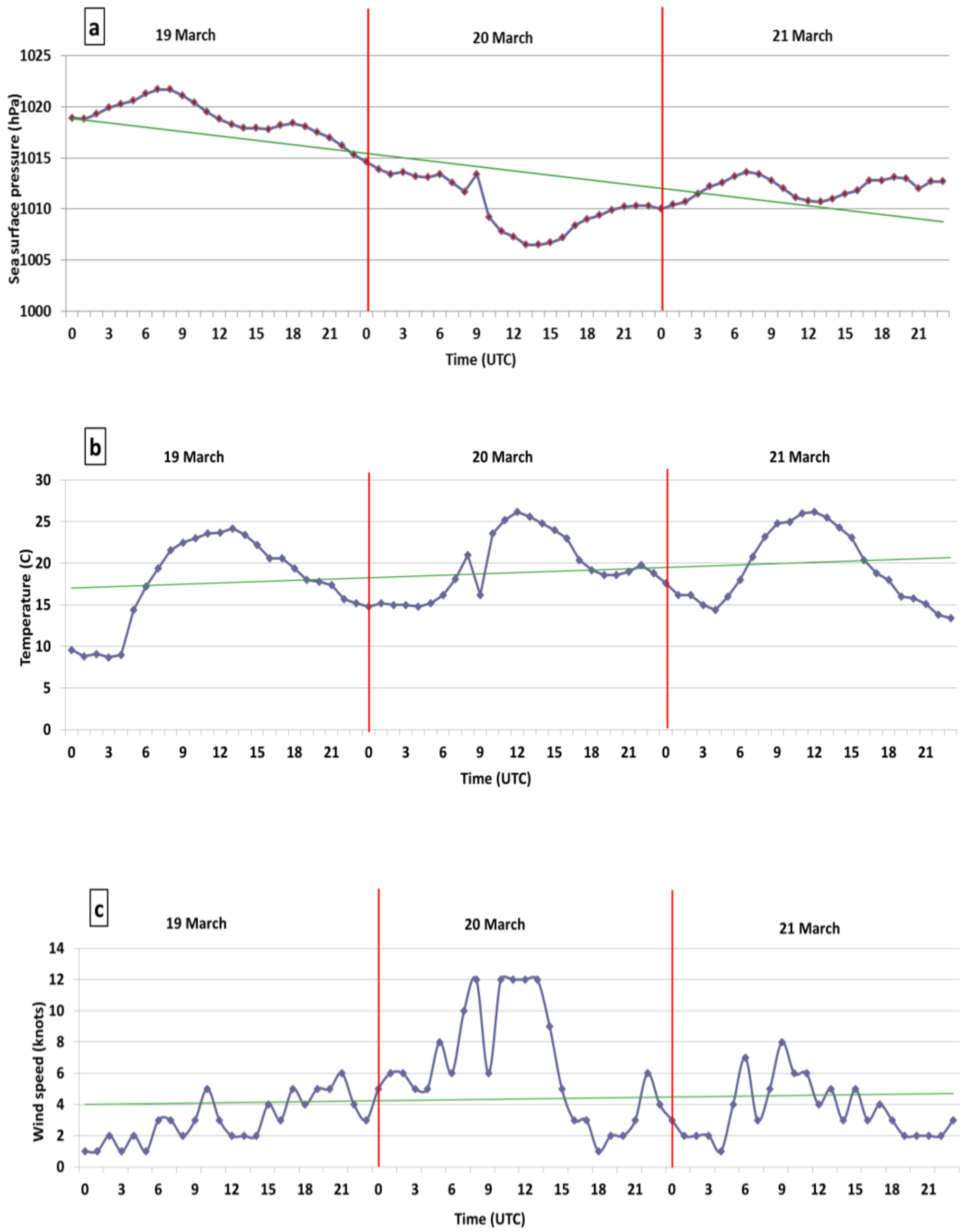

Figure 2- Graphs of hourly values of (a) sea surface pressure, (b) air temperature, (c) and wind speed on three days 19, 20, and 21 March 2016

The synoptic systems and other weather conditions distribution are shown in Figure 3-(a), Figure 3-(b), and Figure 3-(c) at 18 UTC 19 March 0600 UTC, 00 UTC 20 March, and 06 at 20 March 2016. These graphs plotted based on NCEP dataset [31]. In Figure 3-(a), there is a low pressure system moving eastward coming from the Mediterranean Sea to replace the high pressure above Iraq. As the low pressure move more to the east, a close vortex turn to be closed at the western borders of Iraq. The pressure tendency during the previous 6 hours was about 1.7 hPa per hour which is significantly large. At the time of the dust storm (06 UTC) on 20 March (See Figure 3-(c), the low pressure closed system is still spinning on the same area. This setting allows for more emission of dust from the Syrian Desert. As it is clear from the chart, the wind directions are mostly southerly with more than 20 knots.

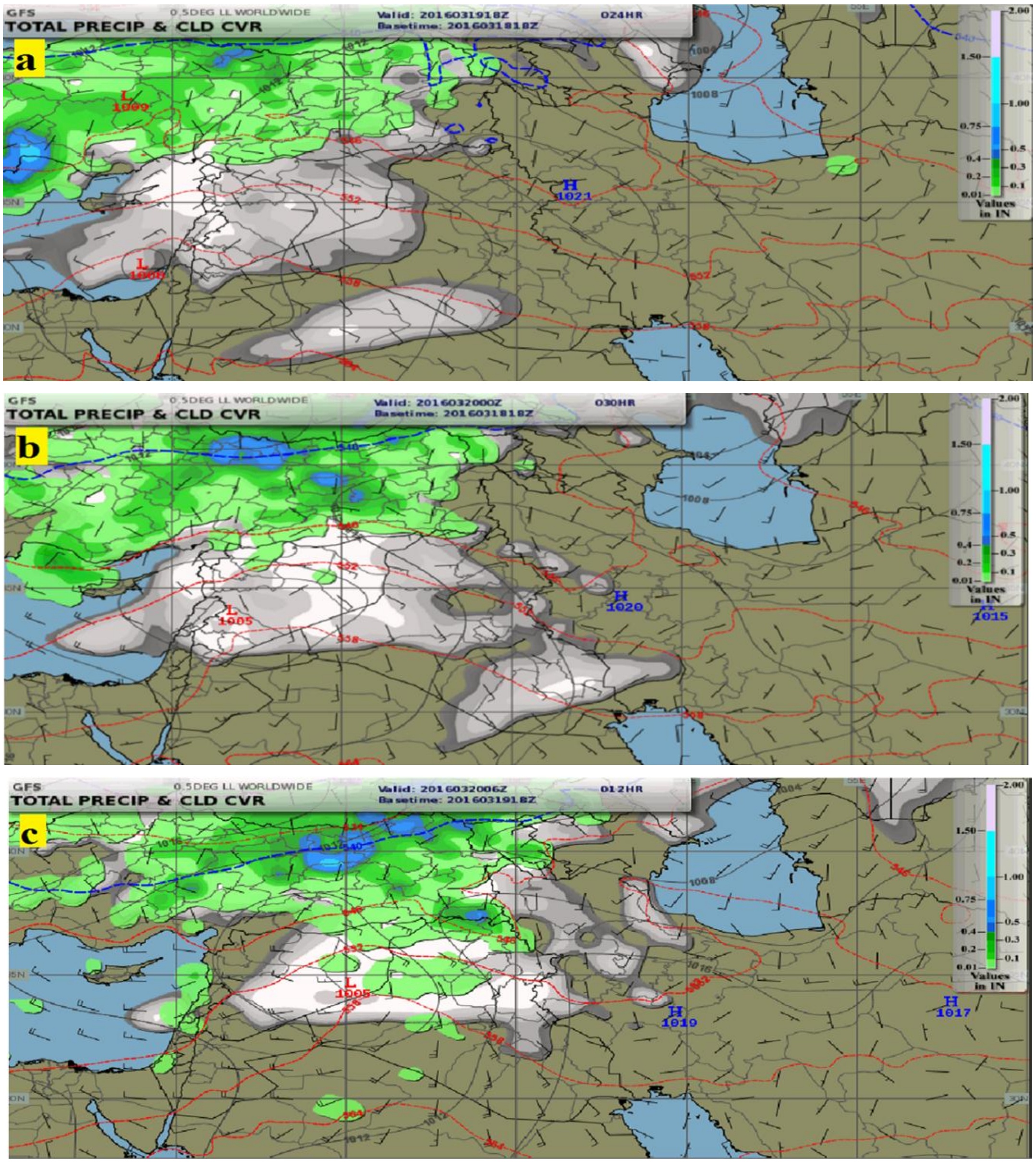

Figure 3- Weather charts of total precipitation and cloud cover (a) at 18 UTC on 19 March 2016, (b) at 00 UTC on 20 March, and (c) at 06 UTC on 20 March. The gray lines refer to the isobars while the red lines refer to the 500 hPa contour lines [31].

During this dust event no significant precipitation was recorded. The pressure gradient was $(20 \times 10^{-3}\ hPa/km)$. The existence of a low pressure system with a cold front offered a near surface mechanism to uptake sand and dust particles from the soil. The high pressure gradient strengthened the wind intensity that assists the dust mobility. The cold front triggered the dust storm by maintaining the horizontal and vertical advection. According to Perrone [32], the southerly flow ahead of the advancing cold front gradually increases in intensity with time as the cold front approaches. These winds activate dust particles in the source region and commence the dust storm process. The turbulence contributed in lifting the dust particles upward. Small particles of dust particles need a high threshold wind value to break the rather strong cohesion force keeping small particles together. At this point, saltation is the dominant mechanism of up taking dust by the wind from the surface. Wind intensity in addition to the arid soil, sedimentary texture, and barren flat area of the west of Iraq together contributed in this dust event.

The prevailing wind during the dust storm was southerly which carried a huge amount of dust to pass through the tunneling track in the Mesopotamia northwestward alongside with Tigris-Euphrates Rivers. The turbulence and vertical advection lifted the fine dust particles upward before its transition through the free atmosphere to distant places from the source area. In Iraq there are many dust sources that could supply the dust storm with additional amounts of dust load, for instance, the region between Tigris and Euphrates rivers south of Baghdad. Because the dominant types of soil in Iraq are clay and silt, which are smaller in size than the sand, the dust would still suspended for more than 24 hours after the dust storm but with lesser concentration. The contour lines in Figure 3-(c) indicate an obvious trough that its axis goes between Crete and Cyprus in the Mediterranean Sea which imprints the existence of surface low pressure exactly above Iraq and suggests the slow movement of the low pressure system.

B. Satellite Imagery

Because most blowing sand and dust occurs over the open desert where there are few, if any, weather reporting stations, forecasting these phenomena was extremely difficult. Satellite imagery is clearly the best way to supplement what few observations there are. In our study, the low pressure system was accompanied by a vast cloud cover which unfortunately obscured an important part of the dust storm underneath. However, the satellite images can give a reasonable overview about the extent of the dust storm. The image from MODIS Dataset (namely, Aeronet) was selected for 20 March 2016 (see Figure-4 [33].

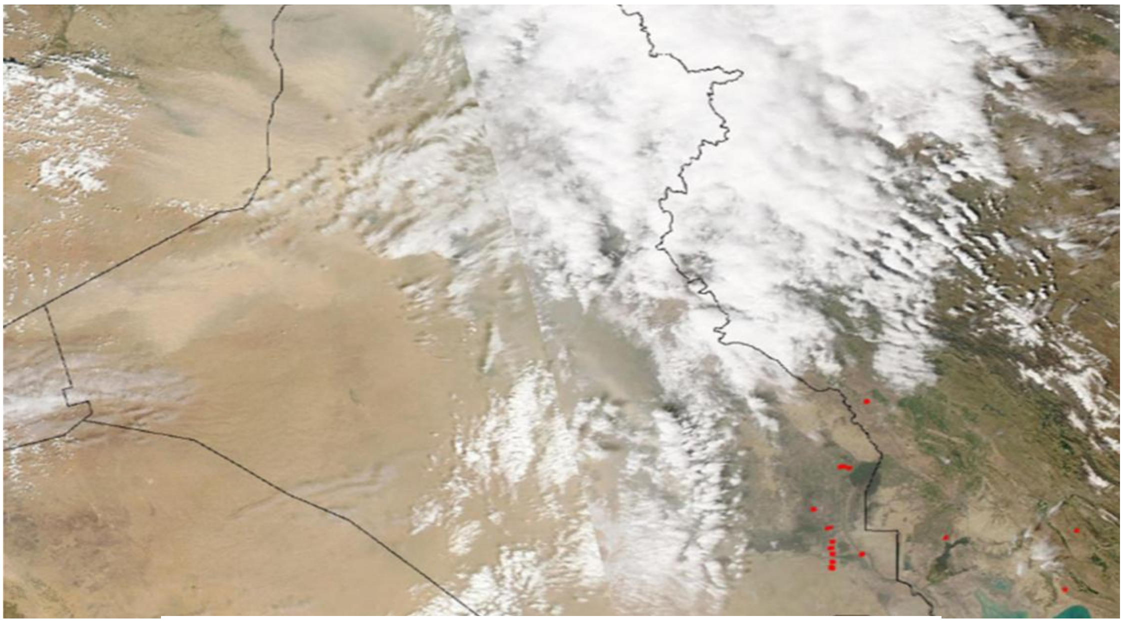

Figure 4-Satellite image of the dust storm for 20 March 2016 [33]

On 20 March, the dust storm was started from the eastern parts of Syria and extended into most of the Iraqi area. It is obvious that the dust storm is thick and easy to notice and discriminate. It is also worth it to say that the dust storm covered a large area which confirms the previous claim that the dust is triggered by a frontal system. Dust storm shape in western of Iraq (Fig.4) gives the impression that the orientation of the wind was northwest and that the source of the dust storm was generated in the east part of Syria.

C. Dust Concentration Analysis

Dust surface concentrations dataset of the NA-ME-E (Northern Africa - Middle East - Europe Regional Center) (2016) was investigated as a reliable alternative of the ground based instruments. Figure-(5) shows a set of charts that visualize the mean values of concentrations for three days (19-21) March 2016 at intervals of 6 or 12 hours [34]. Speaking about Iraq, it is clear from Figure-5 (a) that the dust concentrations were within the range (50-200) $\mu g/m^3$ at 1200 UTC on 19 March 2016 before a large spot of dust began to appear at the west and northwest of Iraq. The cold front passing through agitated the soil in these regions to collaborate the dust storm coming from the Syrian Desert. Figure-5 (b) shows a cloud of thick dust to the west of Thirthar Lake. The concentrations then gradually increased in the morning of 20 March to become within (200-5000) $\mu g/m^3$ commencing from western region which is high value of such parameter. At 1200 UTC, the dust cloud covered most of Iraq with a dust concentration being in the range (200-5000) $\mu g/m^3$. In the morning of 21 March, the effective thick dust cloud begun to move easterly and southeasterly (See Figure-5(c), Figure-5(d), Figure-5(e), and Figure-5 (f)). The nature of the soil particles of Iraq, which is mostly composed of fine clay particles, makes the dust still suspended for few days after the storm, especially under the unstable weather conditions.

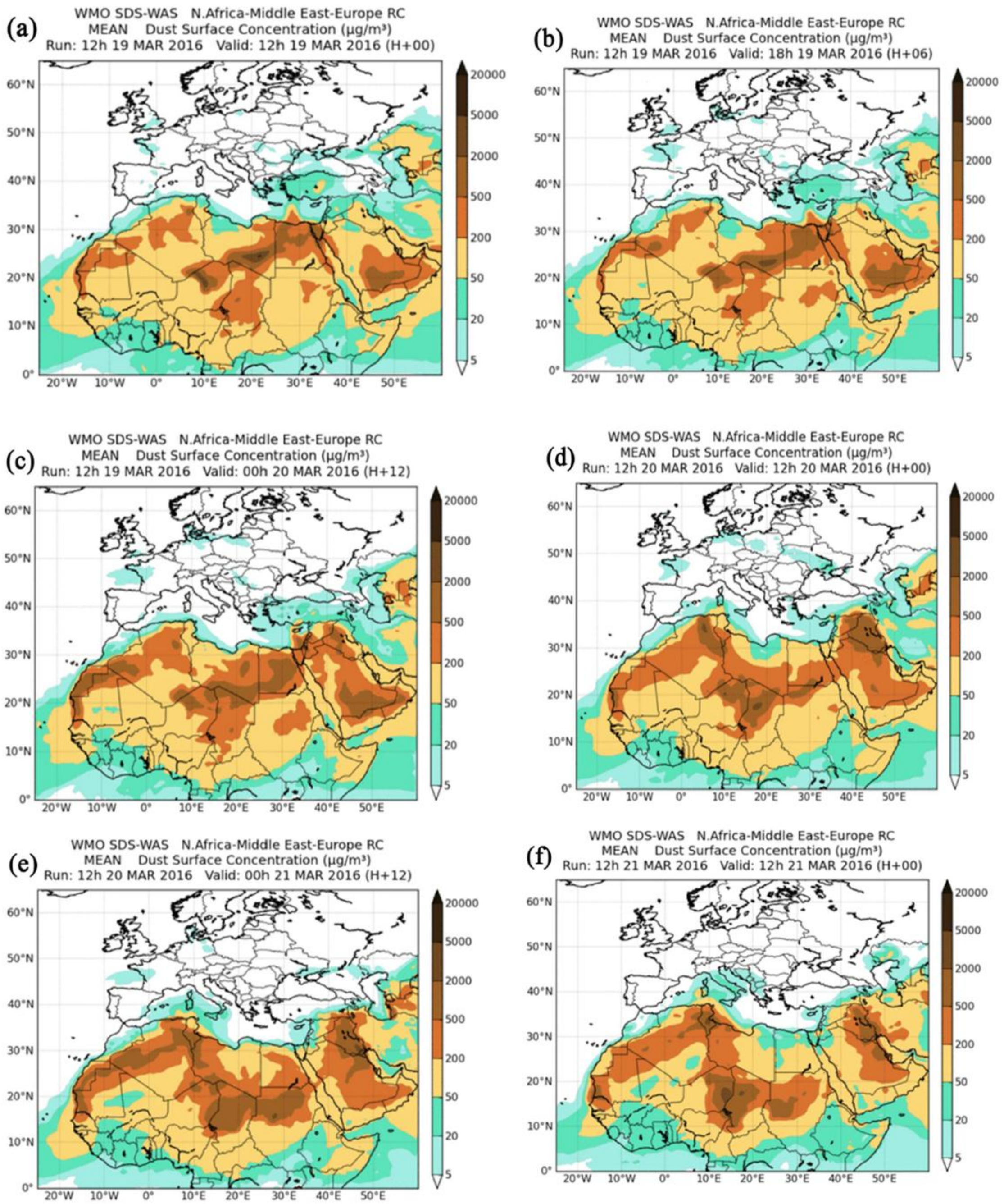

Figure 5- Mean values of dust surface concentration (µg/m^3), (a) 19 March 2016 at 1200 UTC, (b) 19 March at 1800 UTC, (c) 20 March at 0000 UTC, (d) 20 March at 1200 UTC, (e) 21 March at 0000 UTC, and (f) 21 March at 1200 UTC [34].

D. Comparison of the Regional Dust Concentrations

Daily Maximum Dust Concentrations values that were estimated by the four models were used to investigate the dust concentrations for Iraq and some surrounding countries [34]. The values were listed in Table-1 and visualized in Figure-6 (a), Figure-6 (b), and Figure-6 (c) to show how the amount of dust was during the day of the dust storm and one day before and after. Before the outbreak of the dust storm (on 19 March), the daily maximum dust concentrations in Saudi Arabia were larger than the other countries for all models. In 20 March, Iraq's dust concentration values dominated and exceeded the values for the surrounding countries for three models (BSC_DREAM8b, NMMB /BSC-Dust, and NCEP-NGAC). The NMMB/BSC-Dust model made the largest difference. However, the dust concentration values for Iraq and Saudi Arabia became comparable on 21 March except for NMMB/BSC-Dust model.

Table 1-Comparison of daily maximum dust concentration (μg/m^3) of Iraq and some surrounded countries for three days 19, 20, and 21 March 2016 [34]

Date	Country	BSC_DREAM8b (μg/m^3)	NMMB/ BSC-Dust (μg/m^3)	NCEP-NGAC (μg/m^3)	NASA–GEOS-5 (μg/m^3)
19 Mar.	Syria	662	191	868	835
	Jordan	239	153	222	275
	Iraq	779	661	905	1203
	Saudi A.	**1012**	**1351**	**989**	**3584**
	Kuwait	248	97	141	374
20 Mar.	Syria	768	1873	1668	1018
	Jordan	377	576	1211	440
	Iraq	**4256**	**6946**	**2263**	2610
	Saudi A.	1402	2731	2229	**2734**
	Kuwait	2316	2673	2194	2291
21 Mar.	Syria	233	1838	763	262
	Jordan	292	555	223	164
	Iraq	1770	**7872**	1720	**3022**
	Saudi A.	**3078**	2693	**1827**	2224
	Kuwait	1500	2761	1774	2512

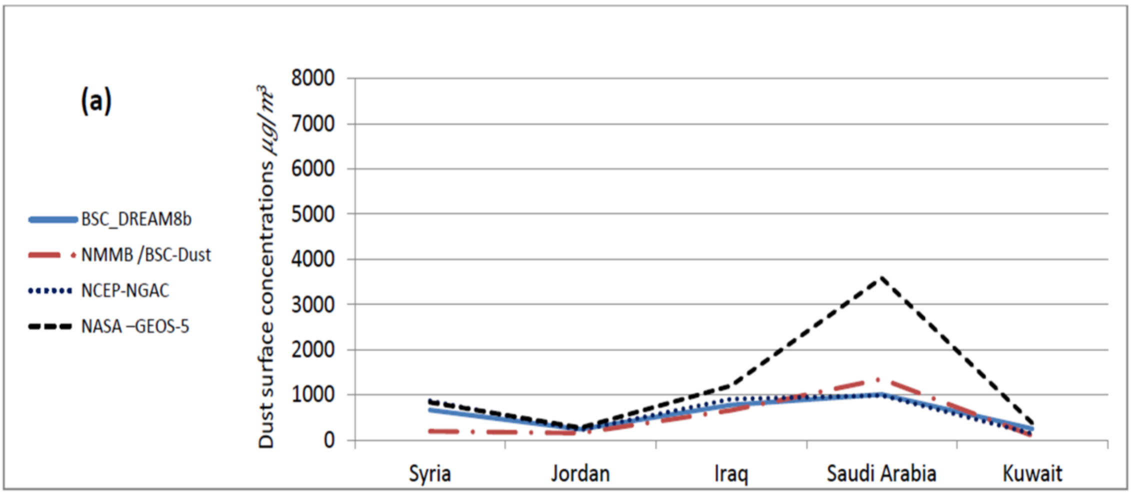

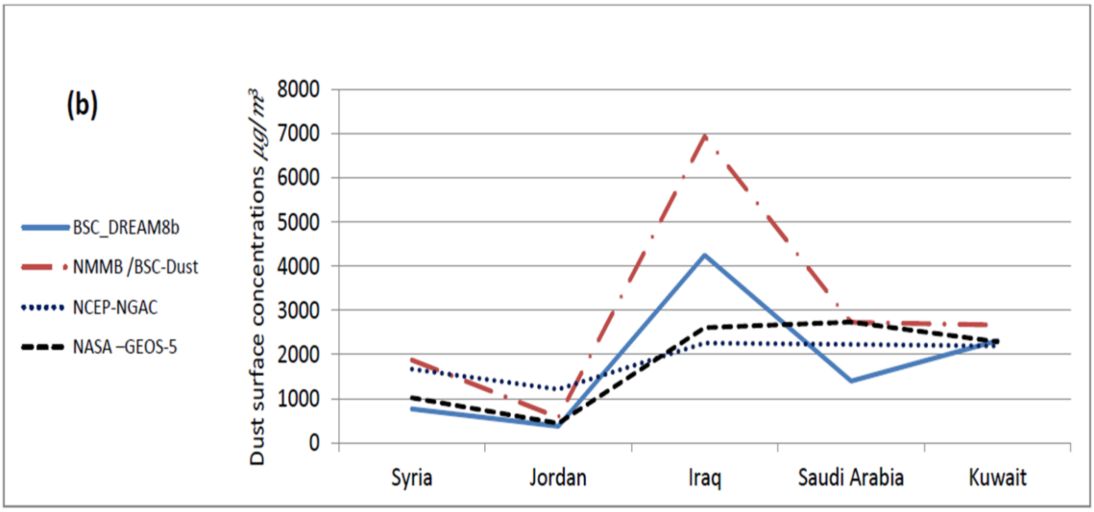

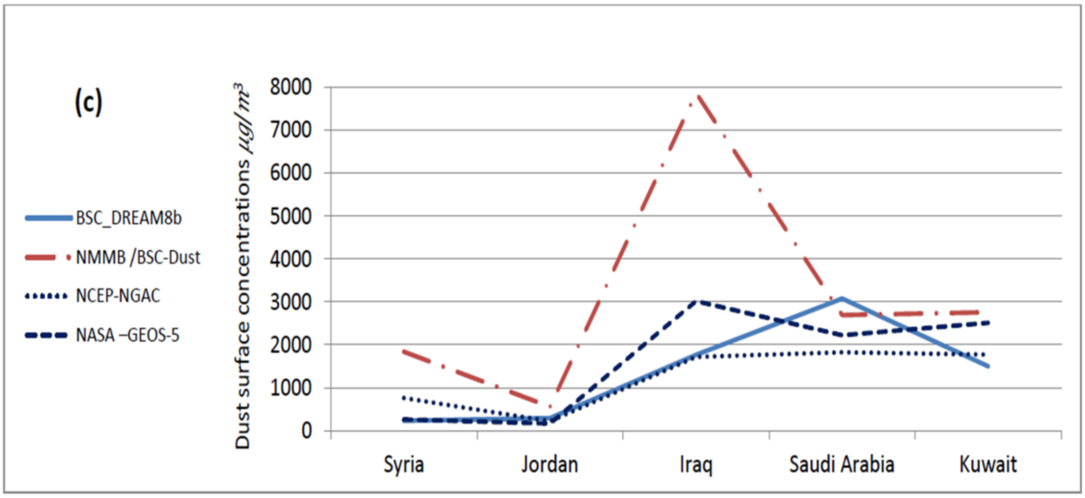

Figure 6-Dust surface concentrations µg/m^3 of some countries around Iraq, (a) on 19 March 2016, (b) on 20 March 2016, and (c) on 21 March 2016 for four models [34].

E. Visibility Reduction

Visibility is one of the most determining factors in describing the dust storms. If the visibility reduces to less than 1000 m due to a dust event, the condition is called a dust storm.

An Experimental relationship between the dust concentration (*C*) and the visibility reduction (D_v) was found by Shao *et al*. [35] for the range of very low visibility under 3.5 *km*:

$$C = 3802.29\, D_v^{-0.84} \quad (1)$$

where *C* is in [μgm^{-3}] and D_v in [km]

According to this relationship, the concentration values corresponding to the visibility reduction can be visualized as in Figure-7.The graph shows that the low visibilities under 0.5 *km* are associated with a large rise in dust concentrations. A value of dust concentration of 3800 μgm^{-3} is associated with a 1000 m visibility. It can be considered this value of concentration above 3800 μgm^{-3} is an indication of the existence of a dust storm. Equation (1) suggests that (BSC_DREAM8b and NMMB /BSC-Dust) models are better in simulation of dust storm values than the others. Hence the equation can be used in Iraq to give approximate estimates of dust concentration in the weather stations that do not have dust concentration measurements.

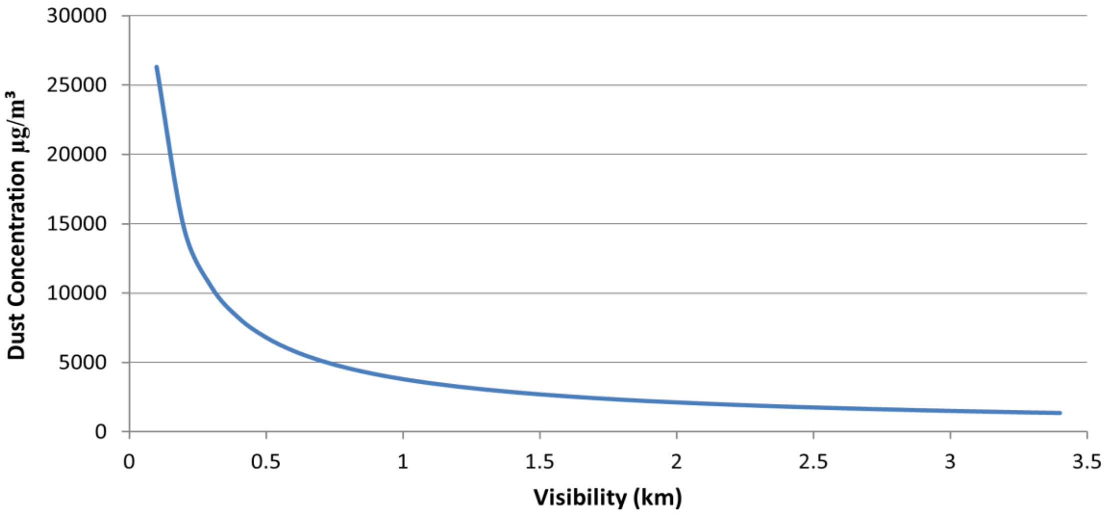

Figure 7- Dust concentration versus visibility.

F. Dust Aerosol Optical Depth Analysis

Measurements of aerosol optical depth (AOD), are based on the fact that the particles change the way the atmosphere reflects and absorbs visible and infrared light. An optical depth of less than 0.1 (palest yellow) indicates a crystal clear sky with maximum visibility, whereas a value of 1 (reddish brown) indicates very hazy conditions [36]. Dust storms obscured the earth surface underneath giving AOD even more than 1.

The aerosol optical depth (AOD) was investigated and analyzed in this study for the same period (19-21 March 2016) for Iraq. As it is clear in Figure-8 [34], the mean values of dust AOD are less than 0.2 on 19 March, reaching 0.4 on the morning of 20 March and then 1.6 at noon which certinly indicating that the dust obsecure the ground. On 21 March the values of mean dust AOD gradually decreases and the cloud of dust move to the south east. The products visualized in Figure-8 are consistent with the satellite images and the situation of the pressure systems.

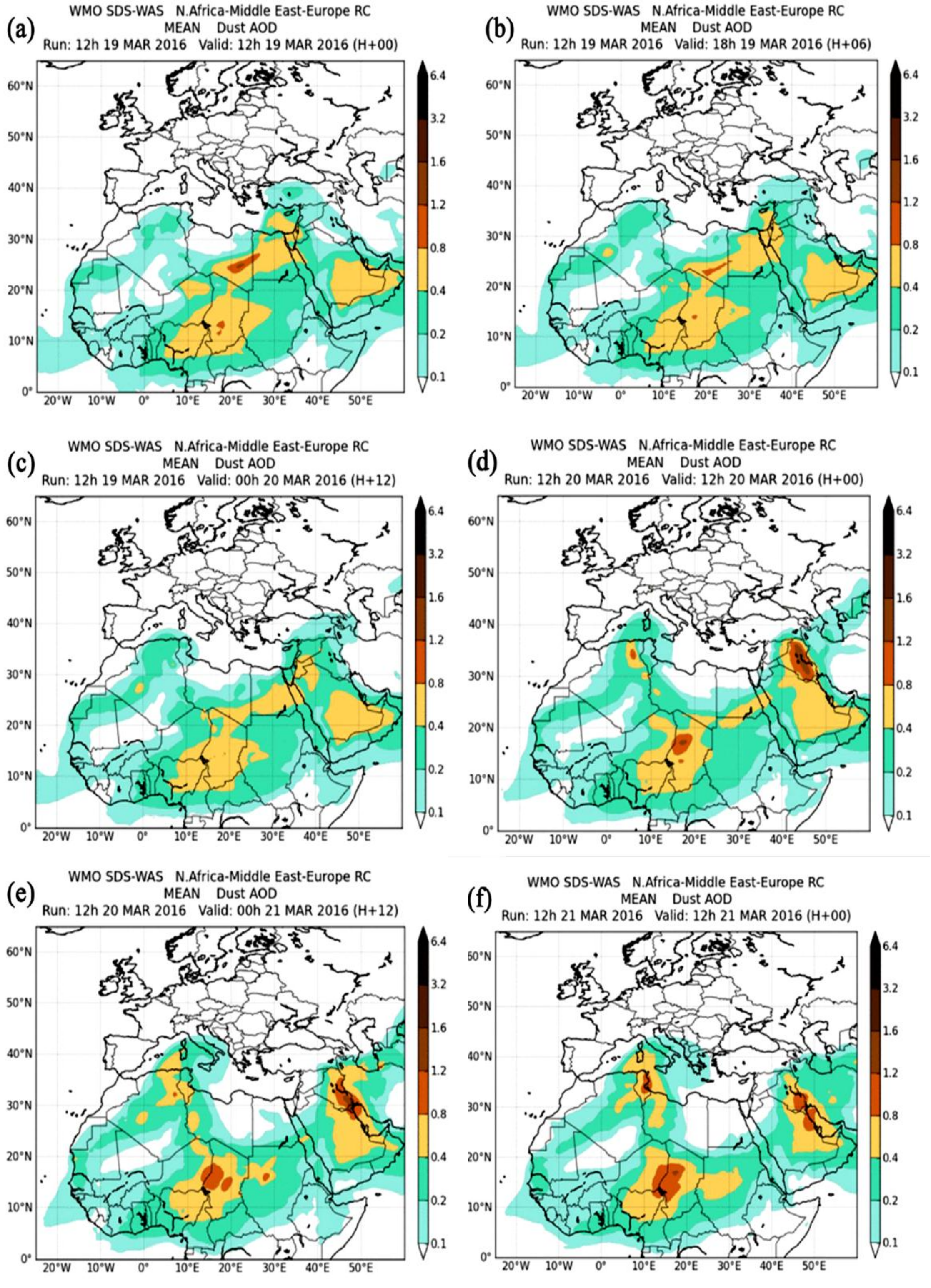

Figure 8-Mean values of dust aerosol optical depth (a) 19 March 2016 at 1200 UTC, (b) 19 March 2016 at 1800 UTC, (c) 20 March 2016 at 0000 UTC, (d) 20 March 2016 at 1200 UTC, (e) 21 March 2016 at 0000 UTC, and 21 March 2016 at 1200 UTC [34].

G. Vorticity and Potential Vorticity

An investigation was made to study the relative vorticity (or shortly "vorticity") and the potential vorticity, as well. The data was acquired from the dataset of the European Center for Medium-Range

Weather Forecasts (ECMWF) [37] and analyzed by Panoply application to display the vorticity and potential vorticity at 500 hPa upper level (see Figure-9 and Figure-10).

Vorticity is a measure of spin about the vertical axis. The positive vorticity is the counter-clockwise rotation and the negative vorticity is the clockwise rotation. The positive vorticity is associated with a vertical uplift of the air in the low pressure system [38]. In Figure-9 the yellow and red colors represent the high positive values of vorticity (cyclonic rotation) whereas the bluish colors refer to the low values of vorticity. The dark blue color refers to the negative vorticity (counter-cyclonic rotation). As it is clear from Fig. 9, that there is an area of high positive vorticity coming from the east of the Mediterranean Sea and moving eastward on 20 March 2016 (Fig. 9 a,b,c). This high positive vorticity is accompanying the upper level trough in our case study. It is well known in meteorology that the surface low pressure system is located to the east of the trough of the 500 hPa upper level. This means implicitly that the surface low pressure system at 06 UTC and 12 UTC on 20 March 2016 is exactly above Iraq. The vorticity is a useful parameter to indicate the shortwave troughs that are embedded within the long waves in the atmosphere. Hence, the pattern of vorticity in Fig. 9 confirms the effectivity of the low pressure system that causes the dust storm. The patterns also show that there is a frontal system which is a robust factor in most of the dust storms.

The potential vorticity is the specific volume times the scalar product of the absolute vorticity vector and the gradient of potential temperature [38]. In Figure-10 the potential vorticity graphs show similar patterns of that of vorticity graphs. However, potential vorticity implies the effect of the surface terrain such as the mountains. In our case study, the Lebanon Mountains must have its own effect. One should take care of the rate of change of the potential vorticity more than the value of the potential vorticity itself since it is associated with the vorticity advection in the downwind flow. In this case study the vorticity advection in the downwind flow is positive and estimated to be about (2.7×10^{-4} K m^2/kg s) along a distance of about 500 km (the distance between the darkest color and the light blue of the vorticity system in Fog. 9b for example. This high value suggests a high positive vorticity advection in the downwind flow and also a high value of divergence east of the system which leads to a significant updraft.

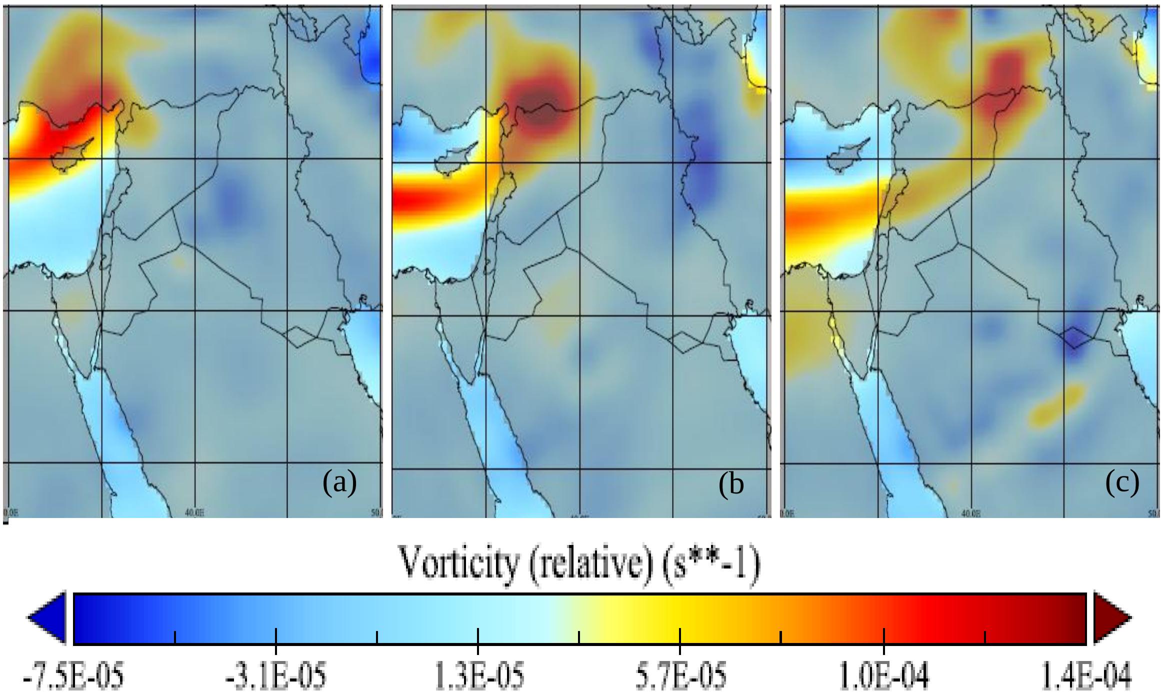

Figure 9- Vorticity at 500 hPa level on 20 March 2016, (a) at 00 UTC, (b) at 06 UTC, (c) at 12 UTC

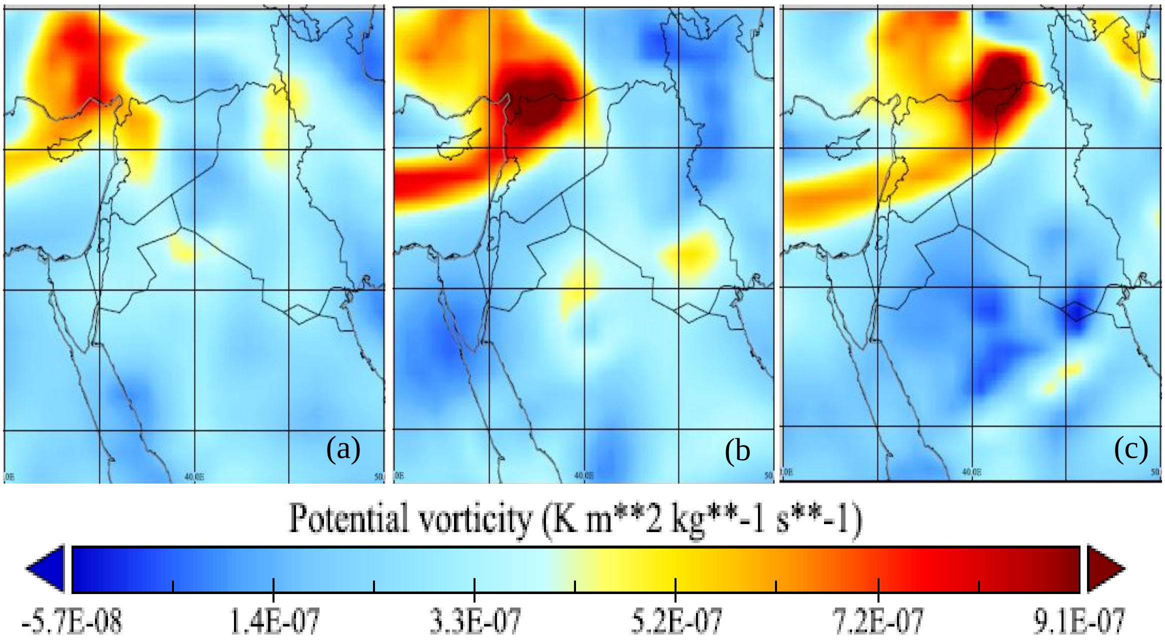

Figure 10-Potential vorticity at 500 hPa level on 20 March 2016, (a) at 00 UTC, (b) at 06 UTC, (c) at 12 UTC

Summary and Conclusions

Dust storms are among the most important phenomena in Iraq and Arabian Peninsula and causes hazardous effects on health and the economic and social activities. In this study a comprehensive case study was conducted to a dust storm that occurred on 20 March 2016. The routinely surface weather data for hourly measurements for three days showed a discontinuity in wind speed, temperature and pressure soundings at the time the front moved above Baghdad. The high pressure gradient and the lifting mechanism achieved by cold front contribute in up taking dust and moving it to distant places. The dust image shows clearly that the dust storm was initiated on the Syrian grounds before entering Iraq with the aid of gradient wind and cold front movement. Dust concentrations and dust aerosol optical depth were also discussed. They simulate the dust storm over Iraq in a reasonable way with some differences. The dust concentrations gradually increased in the morning of 20 March to become within (200-5000) $\mu g/m^3$ which is certainly a high value of such parameter. Testing of the dust concentration by using the products of four models to Iraq and some surrounding countries showed significant increased concentrations in Iraq. An experimental relationship to calculate the dust concentration from visibility data was tested and gave reliable values. Aerosol optical depth (AOD) offered a good means to quantify the dust storm coverage and movement. The values of AOD increased from 0.2 on 19 March to 1.6 at the time of the dust storm which certainly indicating that the dust obscure the ground. Additional investigation was done by using the relative vorticity and the potential vorticity. For relative vorticity, the results show that there is an area of high positive vorticity coming from the east of the Mediterranean Sea and moving eastward. The high value of vorticity in our case study affirms that there are upper shortwaves are responsible of strengthening of the low pressure system in at the surface. Potential vorticity advection was estimated to be about (2.7×10^{-4} K m^2/kg s) along a distance of about 500 km. The high value of positive vorticity advection suggested a high value of divergence east of the system which lead to a significant updraft.

Acknowledgements

We greatly appreciate the efforts of the following agencies: Iraqi Meteorological Organization and Seismology, The Main Center of Meteorology in the Iraqi Air Force, National Aeronautics and Space Administration (NASA), Northern Africa - Middle East - Europe Regional Center, and The European Center of Medium-Range Weather Forecasts (ECMWF) for offering mapping and data of meteorological parameters.

References

1. Buseck, P. R. and Posafai, M. **1999**. Airborne minerals and related aerosol particles: Effects on climate and the environment. Proc. *Natl. Acad. Sci*., **96**: 3372-3379.
2. Solomon, S., Qin, D., Manning, M., Chen, Z., Marquis, M., Averyt, K. B., Tignor, M. and Miller, H. L. **2007**. *Contribution of Working Group I to the Fourth Assessment Report of the Intergovernmental Panel on Climate Change*, 2007, New York, USA, Cambridge University Press.
3. Komeilian, H., Bateni, S. M., Xu, T. and Nielson, J. **2015**. Estimating atmospheric visibility using synergy of MODIS data and ground-based observations, *Remote Sens. GIS Hydrol. Water Resour.*, **368**: 46-50.
4. Knippertz, P. and Todd, M. C. **2012**. Mineral dust aerosols over the Sahara: Meteorological controls on emission and transport and implications for modeling, *Rev. Geophys.*, **50**: 1-28.
5. Xie, J., Yang, C., Zhou, B. and Huang, Q. **2010.** High-performance computing for the simulation of dust storms. *Comput. Env. Urban Syst.*, **34**: 278-290.
6. Schepanski, K., Tegen, I. and Macke, A. **2012.** Comparison of satellite based observations of Saharan dust areas. *Remote Sens. Env.*, **123**: 90-97.
7. Kutiel, H. and Furman, H. **2003.** Dust Storms in the Middle East: Sources of Origin and their Temporal Characteristics. *Indoor Built Env*, **12**: 419-426.
8. Alam, K., Trautmann, T., Blaschke T. and Subhan, F. **2014**. Changes in aerosol optical properties due to dust storms in the Middle East and South Asia. *Remote Sens. Environ*., **143**: 216-277.
9. Choobari, O. A., Zawar-Reza, P. and Sturman, A. **2014.** The global distribution of mineral dust and its impacts on the climate system: A review. *Atmos. Res.*, **138**: 152-165.
10. Middleton, N. J. **1986.** The geography of dust storms, Volume 1. Ph.D. Diss., Oxford University, UK.
11. Nickovic, S., Kallos, G., Papadopoulos, A. and Kakaliagou, O. **2001.** A model for prediction of desert dust cycle in the atmosphere. *J. Geophys. Res.*, **106**: 18113–18129.
12. Sissakian, V. K., Al-Ansari, N. and Knutsson, S. **2013.** Sand and dust storm events in Iraq. *Nat. Sci.*, **5**: 1084-1094.
13. Ginoux, P., Chin, M., Tegen, I., Prospero, J. M., Holben, B., Dubovik, O. and Lin, S. **2001.** Sources and distributions of dust aerosols simulated with the GOCART model. *J. Geophys. Res.*, **106**: 255-273.
14. Hannachi, A., Awad, A. and Ammar, K. **2011.** Climatology and classification of spring Saharan cyclone tracks. *Clim. Dyn*, **37**: 473-491.
15. Wilkerson, W. D. **1991.** *Dust and sand forecasting in Iraq and adjoining countries*, Technical report AWS/TN-91/001, Air Weather Service, USA.
16. Prakash, P. J., Stenchikov, G., Kalenderski, S., Osipov, S. and Bangalath, H. **2015**. The impact of dust storms on the Arabian Peninsula and Red Sea. *Atmos. Chem. Phys*., **15**: 199-222.
17. WMO (World Meteorological Organization). **2013.** *Establishing a WMO Sand and Dust Storm Warning Advisory and Assessment System Regional Node for West Asia: Current Capabilities and Needs*, Technical reports WMO-No., 1121, Geneva, Switzerland.
18. Khaleed, O. L. **2009.** Dust storm Source Areas Determined in Iraq by TOMS and Surface Observations Data. M.Sc. Thesis, Department of Atmospheric Sciences, College of Science, University of Mustansiriyah, Baghdad, Iraq.
19. Khudur, M. H. **2014.** Effects of Dust Storm on Solar Radiation over Iraq. M.Sc. Thesis, Department of Atmospheric Sciences, College of Science, University of Mustansiriyah, Baghdad, Iraq.
20. Al-Dabbagh, S. K. **2015.** Analysis of Dust Events Using BSC-DREAM8b Regional Model and NCEP Data over West Asia (Iraq). Ph.D. Thesis, Department of Atmospheric Sciences, College of Science, University of Mustansiriyah, Baghdad, Iraq.
21. Awad, A. and Mashat, A. **2014,** The synoptic patterns associated with spring widespread dusty days in central and eastern Saudi Arabia. *Atmosphere*, **5**: 889-913.
22. Hamidi, M., Kavianpour, M. R. and Shao, Y. **2013.** Synoptic analysis of dust storms in the Middle East. *Asia-Pacific J. Atmos. Sci.*, **49**: 279-286.

23. Prospero, J. M., Ginoux, P., Torres, O., Nicholson, S. E. and Gill, T. **2002.** Environmental characterization of global sources of atmospheric soil dust identified with the NIMBUS 7 total ozone mapping spectrometer (TOMS) absorbing aerosol product, *Rev. Geophys.*, **40**(2-1)-(2-31).
24. NOAA (National Oceanic and Atmospheric Administration). **2002.** Dust storms, sand storms and related NOAA activities in the Middle East. *NOAA Magazine*, **86**: 1-5.
25. Yu, Y., Notaro, M., Kalashnikova, O. V. and Garay, M. J. **2015.** Climatology of summer Shamal wind in the Middle East. *J. Geophys. Res.*, **121**: 289-305.
26. Vishkaee, F. A., Flamant, C., Cuesta, J., Oolman, L., Flamant, P. and Khalesifard, H. R. **2012.** Dust transport over Iraq and northwest Iran associated with winter Shamal: A case study. *J. Geophys. Res.*, **117**: 1-14.
27. Vishkaee, F. A., Flamant, C., Cuesta, J., Flamant, P. and Khalesifard, H. R. **2011.** Multiplatform observations of dust vertical distribution during transport over Northwest Iran in the summertime. *J. Geophys. Res.*, **116**: 1-17.
28. Bartlett, K. S. **2004.b** Dust storm forecasting for Al Udeid AB, Qatar: An empirical analysis, Dissertation, Air Force Institute of Technology, USA.
29. FAO (Food and Agriculture), **2011.** *Iraq "Country pasture/forage resource profile*, FAO Report, Rome, Italy.
30. Anderson, J. W. **2004.** An analysis of a dust storm impacting operation Iraqi freedom 25-27 March 2003, Dissertation, Naval Postgraduate School, Monterey, California.
31. NCEP (National Centers for Environmental Prediction). **2016.** GFS model charts, provided by The Main Center of Meteorology, Iraqi Air Force.
32. Perrone, T. J. **1979.** *Winter shamal in the Persian Gulf*, Technical Report, Naval Environmental Prediction Research Facility, Monterey.
33. AERONET_Baghdad Subsets. **2016.** https://lance.modaps.eosdis.nasa.gov/imagery/subsets/?project=aeronet&subset=Baghdad.2016080.terra.1km . Accessed 31 December 2016.
34. NA-ME-E (Northern Africa - Middle East - Europe Regional Center) http://sds-was.aemet.es/forecast-products/dust-forecasts. Accessed 12 December 2016.
35. Shao, Y., Yang, Y., Wang, J., Song, Z., Leslie, L. M., Dong, C., Zhang, Z., Lin Z., Kanai, Y., Yabuki, S. and Chun, Y. **2003.** Northeast Asian dust storms: Real-time numerical prediction and validation. *J. Geophys. Res.*, **108**: (3-1)-(3-18).
36. NASA (National Aviation and Aviation Administration). **2017.** Global Maps (2007), (http://earthobservatory.nasa.gov/GlobalMaps). Accessed 8 February 2017.
37. ECMWF (European Center for Medium-Range Weather Forecasts). 2017. ERA Interim, Daily, (http://apps.ecmwf.int/datasets/data/interim-full-daily/levtype=sfc/). Accessed 11 November 2017.
38. Holton, J. R. **2004**. *An introduction to dynamic meteorology*. 4th ed., USA, Elsevier.